Biosystems Engineering 242 (2024) 29–37

Contents lists available at ScienceDirect

Biosystems Engineering

journal homepage: www.elsevier.com/locate/issn/15375110

Research Paper

The development of reference working cycles for agricultural tractors

Leonardo Angelucci, Michele Mattetti *

Department of Agricultural and Food Sciences, Alma Mater Sudiorum, University of Bologna, viale G. Fanin 50, 40127, Bologna, Italy

ARTICLE INFO

Keywords:
Data mining
Real-world data
CANBUS
Efficiency
Engine operating point

ABSTRACT

Climate change and the current energy crisis are creating new challenges to agriculture and new technological solutions must be developed to increase agricultural machinery efficiency. Researchers and machinery manufacturers identified electrified powertrains as a possible solution to meet this demand. The development of field-effective electrified powertrains is challenging mostly due to the wide variability of operating conditions of agricultural tractors. While the automotive industry adopted reference driving cycles for the design and evaluation of hybrid powertrains, the tractor industry has not been able to easily record external load in real-world conditions as it requires dedicated systems that cannot be used under prolonged field usages. This study aims to provide a methodology for estimating a reference working cycle from a multi-year dataset using technologies available in current commercial tractors. Data were collected on a tractor used for 3 years of agricultural work. Data were first clustered into work states, then, for each state, signal features from on-tractor sensors were used to extract key factors to compute the reference work state. With an optimisation solver and a hidden Markov model, the reference working cycle that synthesised the real-world tractor use was calculated. This cycle was compared with established cycles for non-road mobile machinery. The new reference cycle better represented real-world tractor usage as it also complied with low engine operations, which are frequent in farming and mostly associated with machine setup. The new reference working cycle permits a reliable estimation of fuel consumption of real-world farming.

Symbol	Description	Units
a	Tractor longitudinal acceleration	[m s^{-2}]
$a_{e,ae.T}$	Median value of ground acceleration peaks in acceleration events	[m s^{-2}]
d_T	Distance travelled in a task	[km]
EPA	Environmental Protection Agency	[−]
$\mathbf{f}$	Vector of normalised features	[−]
f_*	Generic feature of tasks	[−]
$\widehat{f}_*$	Normalised generic feature of tasks	[−]
$\dot{f}_e$	Engine Fuel Rate	[L h^{-1}]
GHG	Greenhouse gas	[−]
GNSS	Global navigation satellite system	[−]
ICE	Internal combustion engine	[−]
$M_{e\%}$	Actual Engine - Percent Torque	[Nm]
M_f	Nominal friction - Percent torque	[Nm]
M_r	Engine Reference Torque	[Nm]
n_a	Number of acceleration events	[−]
$\mathbf{n_T}$	Array of number of repetitions of reference sub-task	[−]
$n_{T,i}$	Number of repetitions of ith reference sub-task	[−]
NRMM	Non-road mobile machinery	[−]
NRTC	Non-road engine transient cycle	[−]

(*continued on next column*)

(*continued*)

Symbol	Description	Units
P_e	Engine power	[kW]
$\overline{P}_{e,T}$	Median value of engine power in a task	[kW]
$P_{e,ae.T}$	Median value of P_e when acceleration peaks occur	[kW]
PGN	Parameter Group Number	[−]
PTO	Power take-off	[−]
R^2	Coefficient of determination	[−]
RMC	Ramped modal test cycles	[−]
SPN	Suspect Parameter Number	[−]
t_{RC}	Reference cycle constraint	[s]
$\mathbf{t}_{\mathrm{RST}}$	Array of the duration of reference sub-tasks	[s]
t_T	Duration of a task	[s]
V	Tractor ground speed	[m s^{-1}]
$\overline{V}_T$	Median value of ground speed in a task	[m s^{-1}]
ΔV	Ground speed differential in an acceleration event	[m s^{-1}]
ω_e	Engine Speed	[rpm]
$\overline{\omega}_{e,T}$	Median value of engine speed in a task	[rpm]
ω_{fPTO}	Front PTO output shaft speed	[rpm]
ω_{rPTO}	Rear PTO output shaft speed	[rpm]

* Corresponding author.
E-mail address: michele.mattetti@unibo.it (M. Mattetti).

https://doi.org/10.1016/j.biosystemseng.2024.04.004
Received 18 October 2023; Received in revised form 3 April 2024; Accepted 7 April 2024

1. Introduction

The agricultural sector is responsible for about 21% of the world's greenhouse gas (GHG) emissions, primarily due to the use of fossil fuel-based fertilisers and the gas emissions of agricultural machinery (Qiao et al., 2019). The vast majority of self-propelled agricultural machinery is powered by internal combustion engines (ICEs), which are largely run on fossil fuels (Edenhofer et al., 2011). Recently, the European Commission has demanded an extreme reduction in fossil fuel consumption through the approval of the European Green Deal. However, considering the growing world population, a greater production of food is also necessary; thus, it is of utmost importance to achieve what the scientific community denotes as 'sustainable intensification' (Baldoni et al., 2018). The agricultural machinery industry must support this sustainable intensification by developing machines with greater capacity, greater fuel efficiency, and lower GHG emissions. To meet such demands, agricultural machinery manufacturers are following the lead of the automotive industry by pursuing the electrification pathway (Mattarelli et al., 2019; Moreda et al., 2016; Scolaro et al., 2021). Despite the greater complexity of electrified powertrain layouts, electrification maintains the advantage of decoupling external loads from the engine and thus allowing the engine to operate at peak efficiency. Since 2005, tractor manufacturers have been presenting prototypes in major trade fairs for agricultural machinery (Aumer, 2018). The first mild-hybrid tractor to be commercialised was the John Deere 7530 e-Premium, which was equipped with an ICE rated at 150 kW and an electric generator rated at 20 kW for powering accessories (Hahn, 2008). Compared to the equivalent conventional tractor, this solution permitted a reduction of fuel consumption in harrowing and trailer roading by 4% and 16%, respectively (Pessina & Facchinetti, 2009). This tractor was released in 2007 and, despite lower fuel consumption as compared to traditional technology, its production was discontinued two years later, most likely because it did not meet John Deere's market ambitions. The process of electrification of agricultural tractors requires large efforts to develop solutions that can bring real benefits to farmers. To this end, it is necessary to develop powertrains that permit the remedy of operational inefficiencies identified through proper field measurements. These would permit the definition of proper powertrain layouts and sizes for electric machines, or other control strategies (Alberti & Troncon, 2021; Corrochano & Harper, 2016; Rossi et al., 2021; Troncon et al., 2019). However, considering the large variety of operating conditions, designs should not be focused on a limited set of data, but rather on extensive data that include all the main tractor operating conditions (Mattetti et al., 2021).

Over the last 30 years, the automotive industry has pursued this goal with prolonged real-world measurement campaigns aimed at calculating reference driving cycles, which are used to assess the impact of design changes on the performance of components, subsystems or complete vehicles, or to evaluate exhaust emissions (Dembski et al., 2002; Samuelsson et al., 2016). Reference driving cycles have mainly been proposed for road vehicles and are typically represented as a time history of vehicle speed and road grade. Reference driving cycles should portray typical driving conditions; in particular, they should concentrate on overall, real-world vehicle usage (i.e., engine operating points, ranges of speed and acceleration) over a shorter duration (Ashtari et al., 2014). This should be carried out without time-scaling to avoid any artificial or unrealistic alterations (Samuelsson et al., 2016). In the previous literature, several approaches have been reported, most of which are based on the approach developed by André et al. (1995) and Liu et al. (2015).

Scolaro et al. (2021) and Mocera (2021) have pointed out that the lack of reference working cycles is likely to be the major obstacle to tractor electrification, as it complicates the definition of proper specifications for sizing electric drives and energy storage systems. Importantly, the development of a reference driving cycle for agricultural tractors is far more complicated than for passenger cars because the external load is not only dependent on vehicle speed but also on the pulled implement as well as soil and operating conditions (ASAE, 2015; Giakoumis, 2017; Varani et al., 2023). Indeed, engine power may also be required for running different subsystems, such as the power take-off (PTO), hydraulic outlets and the drawbar, and these can furthermore be used either individually or in combination. One of the first studies on the development of reference cycles for non-road mobile machinery (NRMM) was carried out by the United States Environmental Protection Agency (EPA) (Ullman et al., 1999). The results of this study led to the development of several legislative reference cycles, mainly for exhaust emission evaluation, such as the ISO 8178 (ISO, 2017), ramped modal test cycles (RMC) (UNECE, 2010), and non-road engine transient cycle (NRTC) (U.S. Environmental Protection Agency, 2004). The latter has been employed for the measurement of gaseous and particulate matter emissions for Stages III/B in 2011 and IV in 2014 together with the steady-state ISO 8178 C1 (ISO, 2017). NRTC is compliant for a composition of tasks of NRMM (i.e., excavators, backhoes, wheel loaders, etc.), but the portion of the cycle representing a common task carried out by agricultural tractors lasts only 150 s. Landis (2014, pp. 1–8) reported that the NRTC testing procedures did not accurately match typical tractor operating profiles, while McCaffery et al. (2022) used them to evaluate the performance of aftertreatment systems. Recently, a study was published in which a test cycle for determining real-world emissions was proposed (Ettl et al., 2022). Additionally, the German Agricultural Society (DLG, Frankfurt, Germany) developed the DLG-PowerMix (Pieke et al., 2017), which is a set of reference cycles for estimating the potential fuel consumption of agricultural tractor. The set is comprised of 12 field cycles and two transport cycles, with each expressed as a time history of the power delivered by each tractor subsystem (i.e., PTO, hydraulic outlets, drawbar). Each cycle is scaled with a factor depending on the peak PTO power of the tractor being tested. However, DLG-PowerMix does not fully synthesise tractor use, as it does not reproduce all the ancillary activities, such as engine idling, which are frequent in real-world farming (Perozzi et al., 2016; Varani et al., 2022).

Most of these standards and studies have been based on a limited amount of real-world data (e.g., <10 h in the case of the study carried out by Ettl et al. (2022)) due to the supposed low disparity in the operating schedules of NRMM and also because most of these studies were carried out when the costs of data loggers and storage/memory were rather high (Ullman et al., 1999). Nevertheless, Perozzi et al. (2016) monitored a large fleet of agricultural tractors and reported a large variability in operational conditions. This paper aims to fill this knowledge gap by developing a methodology for the construction of a non-legislative reference working cycle for agricultural tractors using a multi-year set of real-world data, which can be used to synthesise a portion of a typical working day over a shorter duration. Here, this cycle will be referred to as a real-world farming cycle (RWFC).

2. Materials and methods

2.1. Data collection

The methodology was applied on the New Holland T7.260 tractor (CNH Industrial, Amsterdam, The Netherlands) whose specifications are reported in Table 1. This tractor is not representative of the fleet of tractors in European farms, but it was chosen for the study since tractors of this class are rich in terms of embedded sensors allowing for comprehensive monitoring of the activity of the different embedded subsystems easing the research.

The tractor was used on the experimental farm of the University of Bologna between October 2018 and November 2021. This farm manages approximately 500 ha of land, of which ~80 ha is devoted to specialty crops and the rest to cereals (mostly, wheat, corn, and sorghum). The same CANBUS data logger used by Mattetti et al. (2021) was installed and set up on the tractor to start recording anytime that the tractor engine was turned on. The tractor was used by a limited number of

Table 1
Specifications claimed by the manufacturer of the tractor used in the study.

Variable [unit]	Value
Engine displacement [c m^3]	6728
Number of cylinders	6
Engine stage	4
Maximum engine power when PTO is engaged [*kW@rpm*]	191@2200
Maximum engine power when PTO is disengaged [*kW@rpm*]	158@2200
Transmission	Full-powershift, 19 gears in forward and 6 in rearward
Engine speed at PTO 540/540E/1000/1000E [rpm]	1931/1598/1912/1583

different professional farmers, and the authors purposefully did not record the driver so as not to interfere with the farming procedures. Thus, farmers were fully unaware of the monitoring process and data were recorded in the most realistic conditions. For this study, only signals with the following Suspect Parameter Numbers (SPNs) and Parameter Group Numbers (PGNs) (ISO, 2012; SAE, 2013) were used for analysis:

- SPN 544 and PGN 65251: '*Engine Reference Torque*' reporting the maximum torque the engine can deliver and denoted as M_r in the following.
- SPN 513 and PGN 61444: '*Actual Engine - Percent Torque*' reporting the torque as a percent of M_r and denoted as $M_{e\%}$ in the following.
- SPN 513 and PGN 5398: '*Nominal friction-percent torque*' reporting the frictional and thermodynamic loss of the engine itself, pumping torque loss and the losses of fuel, oil and cooling pumps as a percent of M_r and denoted as M_f in the following.
- SPN 190 and PGN 61444: '*Engine Speed*' reporting the revolution speed of the engine crankshaft and denoted as ω_e in the following.
- SPN 1883 and PGN 65090: '*Rear PTO output shaft speed*' reporting the speed of the rear PTO and denoted as ω_{rPTO} in the following.
- SPN 1882 and PGN 65090: '*Front PTO output shaft speed*' reporting the speed of the front PTO and denoted as ω_{fPTO} in the following.
- SPN 1877 and PGN 65093: '*Rear hitch in-work indication*' reporting the rear hitch is positioned below (in-work) or above (out-of-work) 85% of the position of the rear three-point linkage (SPN 1873 and PGN 65093).
- SPN 183 and PGN 65266: '*Engine Fuel Rate*' reporting the amount of fuel consumed by engine per unit of time and denoted as $\dot{f}_e$ in the following.
- SPN 1878 and PGN 65094: '*Rear draft*' reporting the horizontal force applied to the lower hitches.

In addition, a GNSS (global navigation satellite system) receiver with an update rate of 10 Hz, with no differential correction and with a purported accuracy of 2.5 m (in terms of circular error probable) (IPE-Speed, IPETronik GmbH, Baden Baden, Germany) was installed in the tractor to monitor its position and its ground speed (V). For consistent time sampling, all signals were resampled at 10 Hz using a cubic spline. From the recorded data, the tractor's longitudinal acceleration (a) was calculated through numerical first-order differentiation of V, while the engine power (P_e) was calculated with Eq. *1*:

$$P_e = M_r \frac{M_{e\%} - M_f}{100} \omega_e \frac{2\pi}{60} \quad \text{Eq. 1}$$

2.2. Data classification

Acquisitions shorter than 5 min were removed from the analysis to avoid the inclusion of any erroneous data coming from ancillary activities caused by the monitoring process or the machinery setup. Using the approach developed by Mattetti, Medici, et al. (2022), data were classified into the following work states: idling, moving and fieldwork with and without the use of PTO. Fieldwork was considered as at minimum a sequence of a pass, a headland, a pass, and another headland turn; the use of PTO was considered to occur when the PTO speed was >0 rpm. The tractor used for the test had an automatic PTO function that automatically turned off the PTO when not needed, so this signal was considered accurate by the authors for discerning PTO applications from non-PTO ones. A time segment in which a certain work state occurred was denoted as a task. For each task, only the portion between two points where the tractor was idle was retained. This avoided the introduction of any artificial points between joined tasks during the cycle reconstruction. Tasks with a retained percentage of lower than 80% were removed and not considered for further analysis. In order to prevent wrongly detected tasks, tasks shorter than a given threshold were removed from subsequent analyses. The adopted thresholds were dependent on the type of work and were: 10 s for idling, 60 s for fieldwork and 300 s for moving. These thresholds were detected through an explanatory analysis of the detected tasks.

For each task, features dependent on the type of work state were calculated and reported as indicated below:

- For all work states:
  - o Median value of engine power ($\overline{P}_{e,T}$).
  - o Standard deviation values of engine power.
  - o Median value of engine speed ($\overline{\omega}_{e,T}$).
  - o Standard deviation value of engine speed.
  - o Median value of ground speed ($\overline{V}_T$).
  - o Duration (t_T).
- For moving states:
  - o Travelled distance (d_T).
  - o Fuel use rate in L/100 km.
  - o Number of acceleration events (n_a) normalised for d_T. Acceleration events were identified as the conditions in which the ground speed differential (ΔV) was >5.5 m s^{-1} in 120 s (Fig. 1).
  - o Median value of ground acceleration peaks in acceleration events ($a_{e,ae.T}$) (Fig. 1).
  - o Median value of P_e when acceleration peaks occur $P_{e,ae.T}$.
- For fieldwork states:
  - o Median value of ground speed during the passes state ($\overline{V}_T$).
  - o For passes with PTO, median speed of the engaged PTOs during the passes state ($\overline{\omega}_{T,PTO}$).
  - o Median value of the rear draft during passes.

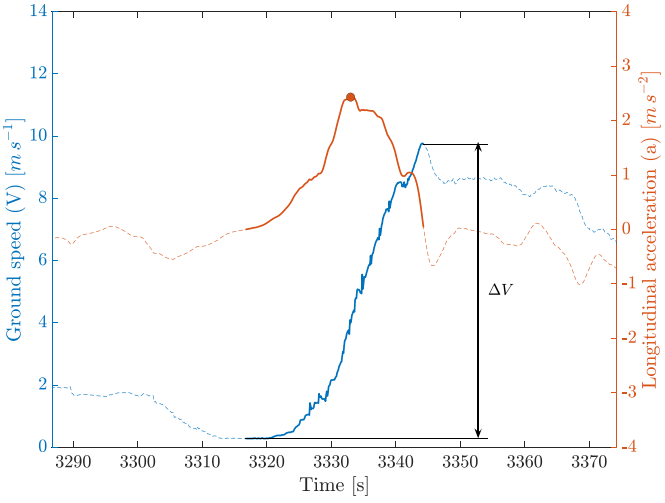

Fig. 1. Ground speed (V) and tractor longitudinal acceleration (a) during an acceleration event and identification of peak acceleration (redpoint). ΔV indicates the speed differential in acceleration events. In the plot, dashed lines were used for entire signals, while the continuous lines were used to highlight the acceleration event.

- Standard deviation of the rear draft during passes.
- Fraction of time spent for the headlands with respect to t_T.

2.3. Determination of reference work states

Considering that the aforementioned features had a different range of values, each feature (f_*) was transformed to fall into a range between 0 and 1 using Eq. (2).

$$\widehat{f}_* = \frac{f_* - \min f_*}{\max f_* - \min f_*} \quad \text{Eq. 2}$$

Thus, each task was characterised by a vector of normalised features (**f**), thereby permitting extraction of the key factors of each task. Each work state was further classified into three work sub-states based on the tertiles of a certain feature. In particular, for idling, moving, fieldwork without PTO, and fieldwork with PTO, the features were t_T, $P_{e,ae.T}/\ a_{e,ae.T}$, $\overline{P}_{e.T}/\overline{V}_T$, and $\overline{V}_T$, respectively. The features used for sub-classification were chosen on the basis of the authors' experience. This sub-classification was carried out to increase the variability of the operating points of the machinery and to spread out the operating points of the engine during the reference working cycle. Considering the limited number of features adopted for task characterisation, and as suggested by Ericsson (2001), no feature selection technique was adopted. For each work sub-state, a representative sub-task was first selected by calculating the pairwise Euclidean distance between **f** of tasks and then calculating the sum of all pairwise distances of a certain task (Fig. 2).

Thus, the selected representative sub-tasks were those that deviated less from all the sub-tasks falling in the same work-state tertile. In Fig. 3, the fieldwork task with the maximum and minimum distance is compared with a set of randomly chosen tasks. It should be noted that all tasks exhibited a similar pattern of $P_{e,}$ with two high level portions occurring during the field passes and two low-level portions occurring during the headlands. Tasks may change in duration, in the contribution of the headlands, and the mean and standard deviation values of P_e during the passes. The task with the minimum distance (blue line in Fig. 3) resembled most of the tasks while the task with the maximum distance (red line in Fig. 3) was significantly different from the rest of the samples.

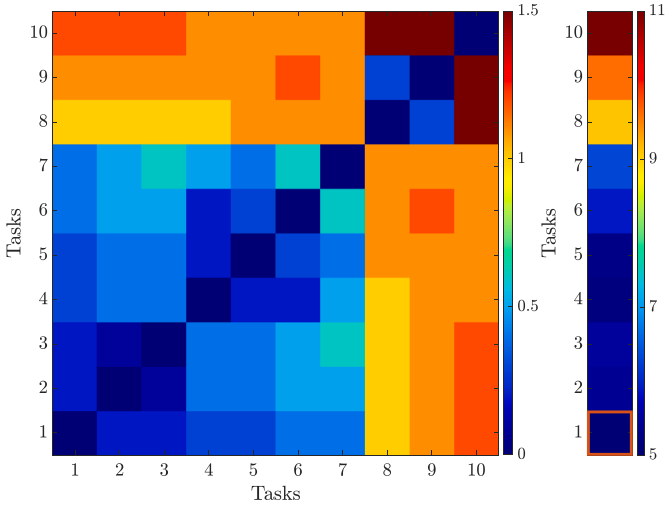

Fig. 2. Example of the approach used for selecting the reference task. On the left is the pairwise distance among tasks, while on the right there is the sum of the pairwise distances of tasks. The task with the lowest sum was selected as the reference task, which is enclosed in the red rectangle in the figure. The colour bars report the values of the distances. (For interpretation of the references to colour in this figure legend, the reader is referred to the Web version of this article.)

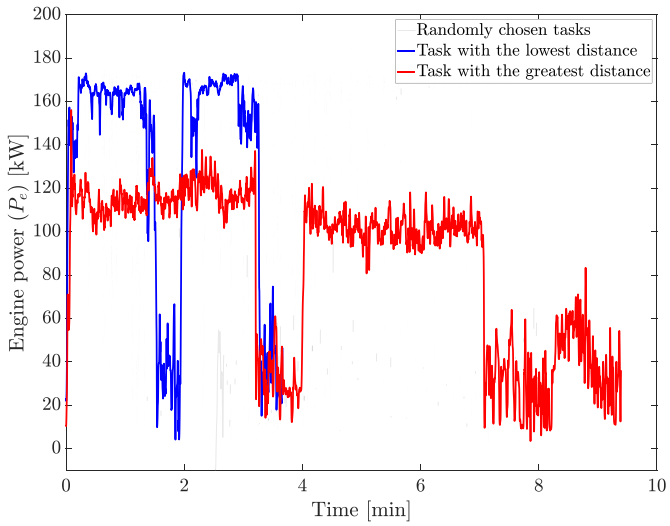

Fig. 3. Time history of engine power (P_e) of a selection of randomly chosen fieldwork without PTO tasks (in grey), as well as sequences with the lowest (blue) and greatest (red) distances. (For interpretation of the references to colour in this figure legend, the reader is referred to the Web version of this article.)

2.4. Cycle construction

Once the reference sub-tasks were identified, their number of repetitions ($\mathbf{n_T}$) were calculated to produce the distribution of P_e of the entire dataset. To this end, the following optimisation problem was defined and solved through a genetic algorithm (Miller, 2000) that was chosen for its ability to solve integer programming problems.

- Design variable: $\mathbf{n_T}$.
- Objective function: Maximisation of the coefficient of determination (R^2) between the probability distribution function of the measured engine power and that of the cycle.
- Constraints:
  - $\mathbf{t}_{RST} \cdot \mathbf{n_T} < t_{RC}$.
  - $n_{T,i} > 1$

where $\mathbf{t}_{RST}$ is the array of the durations of the reference sub-tasks, while $n_{T,i}$ is the number of repetitions of the ith reference sub-task.

Without the first constraint, the optimisation problem solvers were steered towards long cycles to maximise the objective function. Therefore, considering the limited time available for machine development in engineering practice, the first constraint was added in order to limit the duration of the reference cycle to a certain value (t_{RC}). In this study, t_{RC} was considered to be 2 h, as this value was calculated from the collected data, in which it was observed that for 50% of the time the engine was continuously running for less than 2 h.

Once the number of repetitions was calculated, the cycle was stochastically constructed by concatenating the reference sub-tasks in sequence. To do this, the Markov chain model was used. More specifically, the transition probability matrix among work states was calculated and was used to select the subsequent work state for concatenation. Considering that idling tasks were usually shorter than the others, and that tractors were run on idle for a significant amount of time, a large number of repetitions of the reference idling tasks could potentially be obtained. The excess idling reference tasks obtained were equally placed at the ends of the reference cycle as idling is frequent at the ends of the working day (Molari et al., 2019).

3. Results and discussion

The real-world dataset consisted of 982 h of data; the median duration of the tractor workday was 4 h and 44 min. In the dataset, the number of tasks detected were 12,226 of which the percentage classified as idling, moving and fieldwork were 20%, 43%, and 37%, respectively. The median values of the reference sub-tasks for the most meaningful features (according to authors' experience) are reported in Table 2.

Idling reference tasks were the shortest and the work state where the lowest values of P_e were observed. The longer reference tasks were those classified as moving work state, and this may have been caused by the fact that this tractor was used on a farm with fields distributed over a large area, which is a typical layout of farms in the Bologna province (Italy), and where transfers from field to field are common. Indeed, the distance between the two farthest fields is 40 km and the tractor covered ~9000 km year^{-1} driving on roads between fields. The duration of the reference sub-tasks classified as fieldwork was mostly dependent on the pattern of headlands (90% of the headland turns could be classified as fishtail turns (Hunt & Wilson, 2015), length of the field (the 15th and 85th percentiles of field lengths were 40 and 249 m), and ground speed during passes (the 15th and 85th percentiles were 1.3 and 2.5 m s^{-1}). $\overline{P}_{e,T}$ of field works reference tasks were significantly higher than the others. Nevertheless, the moving work state was irregular, with bursts of P_e in acceleration events (Mattetti, Michielan, et al., 2022) leading to values of up to the maximum engine power and, consequently, to a wide range of P_e. Moreover, $\overline{P}_{e,T}$ were correlated with $\overline{V}_T$ due to the fact that, on the road, the largest share of the motion resistance was due to the tyre rolling resistance, both of which are correlated with the tractor's ground speed. Values of $\overline{P}_{e,T}$ for the reference fieldwork tasks were among the greatest and during the headlands, P_e was low (Fig. 3). Thus, the range of P_e in the fieldwork reference task was high where the distinction of P_e between the two operating modes (i.e., field passes and headlands) was clear. Values of $\overline{P}_{e,T}$ in fieldwork with PTO were greater than those of fieldwork without PTO, as when the PTO was engaged, extra power was delivered by the engine (Table 1). For $\overline{\omega}_{e,T}$, the lowest values were observed during idling, while the largest values were observed during field-work. In these conditions, farmers operated where the engine can deliver its peak power. In moving, $\overline{\omega}_{e,T}$ was low because tractors were usually used with high gears and a low load for a better driver comfort and fuel consumption. The values of $\overline{V}_T$ in this work state fell into the typical range for field operations (i.e., between 1.4 and 3.3 m s^{-1}) (ASAE, 2015). It can be seen in Table 2 that, by combining the different reference tasks, the tractor could be made to operate across the entire domain of engine parameters and ground speed.

The typical working day of the tractor was equivalent to a sequence of tasks leading to a field operation (Mattetti, Medici, et al., 2022). This is demonstrated by the transition probabilities between work states (Table 3). The transition probability 'from idling to moving' was much greater than that of 'from idling to fieldwork'. This is because idling mostly occurs around farm building for activities such as implement hitching, or machine servicing. In this condition, the only possible subsequent tractor state is moving due to the on-road transfer to a field. When a tractor leaves the road, it then enters a field and the equipment setup is usually changed (i.e., the implement must be adjusted from the transport mode to an operational mode). This forces the operator to halt the tractor, leading to an intermediate idling task. An idling stop should also occur when a field has been processed and the driver stops the tractor to change the implement operating mode (i.e., from an operational mode to the transport mode). So, 'from idling to moving' transitions occur when leaving farm buildings and when leaving fields, while 'from moving to idling' transitions occurs only when entering fields and this should explain the higher transition probability of the 'from idling to moving' than 'from moving to idling'. This may explain why the transition 'from moving to idling' was more frequent than that of 'from moving to fieldwork'. Even if fieldwork tasks were interrupted by an idling task for implement adjustment (Molari et al., 2019), the transition from fieldwork to moving was more frequent than that from fieldwork to idling, as tractors may work on large fields separated by drain channels. This process also interrupted a fieldwork task with a moving one.

In Fig. 4, the comparison between the probability density function of P_e of the dataset with respect to that of the RWFC is reported. It can be seen that the two distributions have a high similarity. Indeed, the resulting R^2 between the two functions was 0.74 and, they were similar in shape since both exhibited a multimodal distribution. In particular, the global maximum value was 5 kW, mostly occurring during the idling phase. The other local maximums for the dataset were 168 and 188 kW, occurring mostly on the 2nd and 3rd quartiles of passes with PTO, respectively (Table 2). Moreover, the overlapping area of the two distributions was 83%, indicating a high similarity between the two.

The dataset and RWFC were compared with NRTC and EPA cycles, which are commonly used for NRMM (Giakoumis, 2017). The EPA cycle predominantly resembled a typical field operation, with a limited amount of idling and a sequence of field passes, headland turns, and field passes. Thus, in the cycle, there were two high-load portions as well as a lower one (Fig. 5a). The NRTC is a legislative cycle for NRMM engines comprising earthmoving machinery operations (Fig. 5b). In these operations, bursts of load are common, especially for excavators, and these were observed in the cycle around minute 13. However, the RWFC included only agricultural operations with different levels of intensity where, unlike in other applications, idling portions of different durations were distributed over the cycle.

In Fig. 6, the probability histograms between ω_e and P_e are reported. It can be seen that, during the monitoring period, the engine was operated over the entire operating domain; the greatest probability occurred when the engine speed and power were very low during idling. Moreover, the tractor was operated for a significant amount of time in the range of engine speeds between where the peak torque and the peak power occurred (i.e., 48%). This can also be observed for the RWFC distribution (Fig. 6d) but not for the EPA and NRTC cycles. Indeed, in these two cycles, but especially for EPA cycle, only a limited part of the domain of engine parameters is covered. For the EPA cycle, engines mostly operate in idling and around maximum power region; while on for NRTC, engines also operate for a significant amount of time in partial

Table 2
The most meaningful features for each reference sub-task.

Work state	t_{RST} [s]	$\overline{P}_{e,T}$ [kW]	$\overline{\omega}_{e,T}$ [rpm]	$\overline{V}_T$ [m s^{-1}]
Idling	20	4	850	0.0
	75	5	850	0.0
	403	5	850	0.0
Moving	1118	58	1417	7.9
	464	39	1444	5.1
	472	42	1771	6.6
Fieldwork without PTO	236	111	1853	2.1
	175	164	2071	2.1
	206	150	2140	1.6
Fieldwork with PTO	321	152	1873	0.9
	317	168	1896	1.1
	213	188	1945	1.6

Table 3
Transition probabilities between work states.

		To		
		Idling	*Moving*	*Field work*
From	*Idling*	0	0.8136	0.1864
	Moving	0.6883	0	0.3117
	Fieldwork	0.3328	0.6672	0

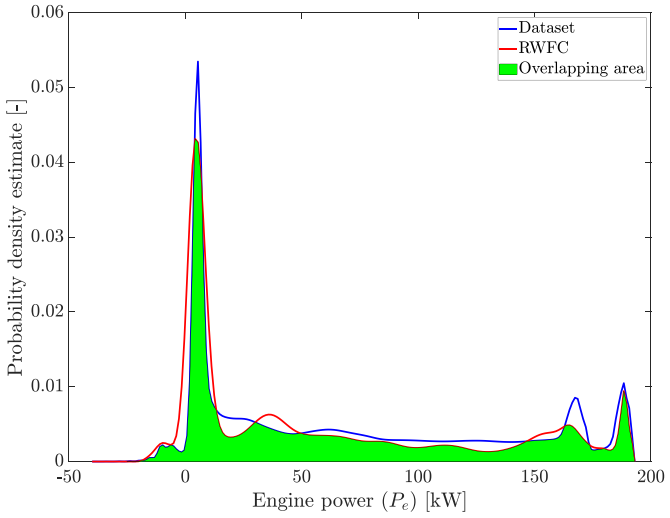

Fig. 4. Comparison between the probability density functions of the engine power (P_e) of the dataset and the RWFC. The green area indicates the overlapping area between the two distributions. (For interpretation of the references to colour in this figure legend, the reader is referred to the Web version of this article.)

load conditions. Moreover, the values of the probability of the dataset and RWFC were significantly lower than those observed for EPA and NRTC cycles, as data were spread out over a greater number of bins.

Considering that all cycles had significantly different durations, basic statistics of engine-related parameters were calculated (Table 4) to perform a quantitative comparison between the dataset and all cycles.

Table 4 highlights the large difference between the two established cycles (i.e., EPA and NRTC) with respect to the dataset. By comparing the mean fuel consumption for the EPA cycle with that of the dataset, the former differed from the latter by 71%, and it can immediately be deduced that the EPA cycle does not represent the usage of the tractor within this study. This large difference in the EPA cycle was caused by the fact that it represented only heavy load operations, which represents less than 50% of the use of this class of tractors in Italy (Mattetti et al., 2021). Furthermore, since the deviation of the mean fuel consumption of NRTC compared to that of the dataset was only 7%, it can be deduced that the NRTC cycle faithfully reproduced tractor usage in this study. However, by analysing the other statistics reported in Table 4, the NRTC was not overall able to reproduce the real-world tractor usage due to its inability to reproduce low-demand engine operations. Indeed, the idling period in the EPA and NRTC cycles was approximately five-fold lower than that shown in this study's dataset. Moreover, the NRTC included two idling phases, lasting for 23 and 25 s, respectively, but idling stops could be much longer than this (Molari et al., 2019), leading to potentially higher specific fuel consumption and exhaust emission levels than those occurring in real-world farming (Rahman et al., 2013). Furthermore, the distribution parameters (i.e., values of 10th, 50th, and 90th percentiles) of ω_e, T_e, and P_e and their gradients were significantly different than those of this study's dataset. In particular, the 50th percentile of ω_e in the NRTC and EPA cycles were respectively 17% and 39% greater than that occurring in this dataset. Moreover, the 90th percentile of ω_e of the NRTC and EPA cycles were respectively 17% and 2% greater than their 50th percentile values, which were lower than that of the dataset (i.e., 26% greater than its 50th percentile). This difference indicated the different distributions of ω_e of both cycles, which were, especially for EPA, significantly more left skewed than that of the dataset. This is the consequence of the fact that both cycles were mainly comprised of only very high and very low engine load portions. This differs from real-world farming, where engines of agricultural tractors operate at a different range of ω_e due to the different operating demands. For example, during PTO field operations, the engine should be run at

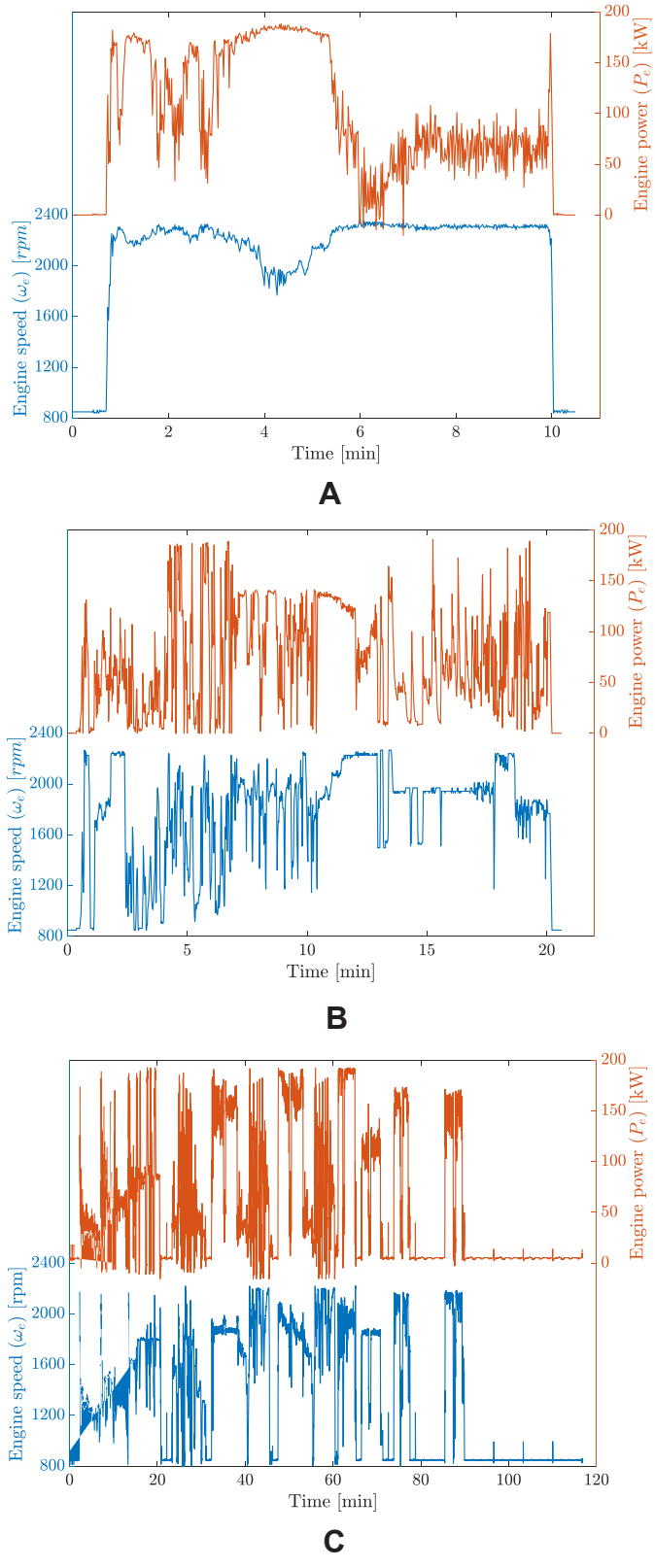

Fig. 5. The temporal trend of engine speed (ω_e) and engine power (P_e) of (a) the EPA, (b) the NRTC, and (c) the RWFC cycles.

the nominal speed of the PTO in operating mode (i.e., standard or economy) (Table 1). On the other hand, for tillage and moving operations, the engine usually runs at a speed between that of the peak engine torque and power in order to maximise tractor driveability. With respect

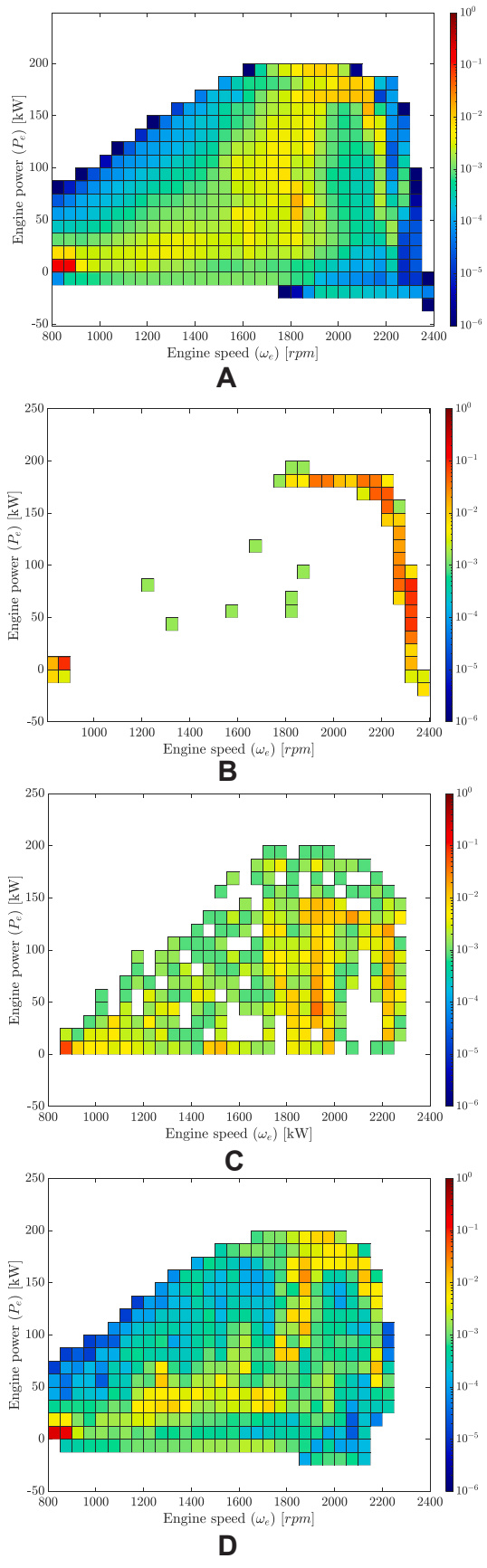

Fig. 6. Probability density histogram between engine speed (ω_e) and engine power (P_e) for (a) the entire dataset, (b) the EPA cycle, (c) NRTC (the third from the top), and RWFC.

Table 4
Comparison between basic statistics of engine-related parameters of the dataset with EPA, NRTC, and RWFC.

Parameter	Dataset	EPA	NRTC	RWFC
Duration [min:ss]	58,924:00	10:20	20:38	116:44
Idling period [in % with respect to the entire duration]	25	6	5	36
Mean fuel consumption [$L\,h^{-1}$]	17.4	29.7	18.6	14.0
Engine speed: $10^{th}/50^{th}/90^{th}$ percentiles [rpm]	849/1629/2058	860/2276/2324	1052/1903/2226	850/1290/2009
Engine power: $10^{th}/50^{th}/90^{th}$ percentiles [kW]	5/50/169	0.4/82/181	6/65/137	4/30/163
Engine torque: $10^{th}/50^{th}/90^{th}$ percentiles [Nm]	57/298/846	4/341/846	55/336/687	48/198/816
Gradient of the engine speed: $10^{th}/50^{th}/90^{th}$ percentiles [rpm s^{-1}]	−63.6/0.0/64.8	−16.7/0/16.9	−101.2/0/85.7	−46.4/0.0/42.6
Gradient of the engine torque: $10^{th}/50^{th}/90^{th}$ percentiles [Nm s^{-1}]	−109.5/0/113.5	−60.6/0/60.20	−122.0/0/122.3	−82.5/0/84.1
Gradient of the engine power: $10^{th}/50^{th}/90^{th}$ percentiles [kW s^{-1}]	−16.8/0/17.6	−13.7/0/14.0	−22.1/0/23.1	−12.5/0.0/13.4

to the dataset, the 50^{th} and 90^{th} percentiles of P_e of the NRTC cycle were greater than that of the dataset of 15 and 32 kW, which corresponded to 8% and 18% of the peak engine power, respectively. For the EPA cycle, the 50^{th} percentile of P_e of was 32 kW greater than that of the dataset. Moreover, the 10^{th} percentile of the EPA cycle was almost 0 kW because in the idling phase of the EPA cycle the engine power is 0 kW. This is unrealistic, as during idling, the engine drives accessories that demand up to 4 kW of power for this type of tractor (Saetti et al., 2021). During the EPA cycle, the engine operated in a less transient operating condition than that which occurs in real-world farming conditions. This can be observed by comparing the statistics of gradients of ω_e, T_e and P_e, which were significantly lower in absolute value than those of the dataset. The NRTC cycle is slightly more transient than the dataset; indeed, the gradients of ω_e, T_e and P_e were, in absolute value, up to 59%, 31%, and 12% greater than that of the dataset, respectively. This was probably caused by the fact that the NRTC cycle was also designed for earth-moving machinery operations that are notoriously more transient than agricultural ones. Thus, these results demonstrated that the EPA and NRTC cycles were not fully representative of real-world tractor usage, and therefore should be used with prudence for evaluating GHG emissions or the potential fuel consumption of agricultural tractors. On the other hand, the RWFC represented a combination of certain portions of the dataset; thus, deviations for most of the statistics when compared to those of the dataset were generally lower than those of EPA and NRTC cycles.

The cost of better representativeness of the RWFC with respect to other cycles was a comparatively longer duration of the cycle with respect to established cycles. Indeed, most of the cycles in use for vehicle testing are typically shorter than an hour (Giakoumis, 2017). However, in order to increase the representativeness of cycles with respect to real-world driving, they have been extended in the last decades. Indeed, the ECE-17 adopted in Europe between 1970 and 2017 for passenger cars was limited to 800 s, while the current cycle (i.e., WLTC) lasts 1800 s. Therefore, the greater duration of RWFC than the other cycles in use should not be considered a critical factor in a modern context where a reliable estimation of fuel consumption and GHG emissions is of primary importance.

Although the developed cycle proposed here was based on data collected from a single tractor, the representativeness of the reference cycle could be increased by employing the same methodology on an enlarged, real-world dataset. Another future development in this line of research would be the calculation of a tractor class-independent working cycle by scaling engine parameters, as has been carried out for the EPA and NRTC cycles. Moreover, it would be beneficial for farming to develop a European working cycle, such as that created for passenger cars. However, considering that agriculture is characterised by regional practices, it will be a challenge to create a working cycle that includes all the uses, and will require a very large dataset based on real-world usage.

4. Conclusions

The automotive industry has demonstrated that driving cycles can be used for many purposes, such as refinement of vehicle design, estimation of fuel use and emission control. In agricultural engineering, very few studies have investigated such topics, and the design of novel machinery is still based on old rules or assumptions. However, the growing interest in tractor electrification will require novel approaches for designing efficient tractors in farming applications and this will require a reference tractor working cycle. Here, the first wholistic tractor-specific reference working cycle was developed using a CANBUS data analytics approaches applied to data collected from a single tractor operated over 3 years on a mixed cropping enterprise near Bologna, Italy. The new reference cycle was shown to outperform other machinery reference cycles, in particular in its ability to account for idling processes that are typical in farming operations. The development of better tractor-specific driving cycles will permit engineers to steer the design of machinery, including machinery with electric motors, towards more realistic operating conditions, potentially resulting in more efficient tractors.

CRediT authorship contribution statement

Leonardo Angelucci: Formal analysis, Methodology, Visualization. **Michele Mattetti:** Conceptualization, Methodology, Resources, Supervision, Writing – original draft, Writing – review & editing.

Declaration of competing interest

The authors declare that they have no known competing financial interests or personal relationships that could have appeared to influence the work reported in this paper.

Acknowledgements

The data collection of this project was supported by MUR (Ministry of University and Research) under the 2017 PRIN (Research Projects of Significant National Interest) call notification '*Green SEED: Design of more-electric tractors for a more sustainable agriculture*', grant number: 2017SW5MRC. Data analysis was carried out within the Agritech National Research Center and received funding from the European Union Next-GenerationEU (PIANO NAZIONALE DI RIPRESA E RESILIENZA (PNRR) – MISSIONE 4 COMPONENTE 2, INVESTIMENTO 1.4 – D.D. 1032 June 17, 2022, CN00000022). This manuscript reflects only the authors' views and opinions; neither the European Union nor the European Commission can be considered responsible for them.

References

Alberti, L., & Troncon, D. (2021). Design of electric motors and power drive systems according to efficiency standards. *IEEE Transactions on Industrial Electronics, 68*(10), 9287–9296. https://doi.org/10.1109/TIE.2020.3020028

André, M., Hickman, A. J., Hassel, D., & Joumard, R. (1995). *Driving Cycles for emission measurements under European conditions (SAE technical paper 950926)*. *SAE international*. https://doi.org/10.4271/950926

ASAE. (2015). *Asae EP496.3—agricultural machinery management*. Standard: ASAE.

Ashtari, A., Bibeau, E., & Shahidinejad, S. (2014). Using large driving record samples and a stochastic approach for real-world driving cycle construction: Winnipeg driving cycle. *Transportation Science, 48*(2), 170–183. https://doi.org/10.1287/trsc.1120.0447

Aumer, W. (2018). *Funktionsintegration elektrischer antriebe in mobilen arbeitsmaschinen. Fortschritte naturstofftechnik*. Springer. https://doi.org/10.1007/978-3-662-57457-7_5

Baldoni, E., Coderoni, S., & Esposti, R. (2018). The complex farm-level relationship between environmental performance and productivity: The case of carbon footprint of Lombardy farms. *Environmental Science & Policy, 89*, 73–82. https://doi.org/10.1016/j.envsci.2018.07.010

Corrochano, D. G., & Harper, L. (2016). Challenges of hybridisation of off-highway machinery. In *6th hybrid and electric vehicles conference (HEVC 2016)* (pp. 1–7). https://doi.org/10.1049/cp.2016.0962

Dembski, N., Guezennec, Y., & Soliman, A. (2002). *Analysis and experimental Refinement of real-world driving cycles (SAE technical paper 2002-01–0069)*. SAE International. https://doi.org/10.4271/2002-01-0069

Edenhofer, O., Pichs-Madruga, R., Sokona, Y., Seyboth, K., Kadner, S., Zwickel, T., Eickemeier, P., Hansen, G., Schlömer, S., von Stechow, C., & Matschoss, P. (2011). *Renewable energy sources and climate change mitigation: Special report of the intergovernmental panel on climate change*. Cambridge University Press. https://doi.org/10.1017/CBO9781139151153

Ericsson, E. (2001). Independent driving pattern factors and their influence on fuel-use and exhaust emission factors. *Transportation Research Part D: Transport and Environment, 6*(5), 325–345. https://doi.org/10.1016/S1361-9209(01)00003-7

Ettl, J., Emberger, P., Thuneke, K., & Remmele, E. (2022). Practical tractor driving cycles for determining real emissions. *ATZheavy Duty Worldwide, 15*(1), 10–15. https://doi.org/10.1007/s41321-022-0481-3

Giakoumis, E. G. (2017). *Driving and engine cycles*. Springer International Publishing. https://doi.org/10.1007/978-3-319-49034-2

Hahn, K. (2008). High voltage electric tractor-implement interface. *SAE International Journal of Commercial Vehicles, 1*(1), 383–391. https://doi.org/10.4271/2008-01-2660

Hunt, D., & Wilson, D. (2015). *Farm power and machinery management* (11th ed.). Waveland Press.

ISO. (2012). *ISO 11783-7:2012—tractors and machinery for agriculture and forestry—serial control and communications data network—part7: Implement messages application layer—implement messages application layer*.

ISO. (2017). ISO 8178-4: Reciprocating internal combustion engines. Exhaust emission measurement. Steady-state and transient test cycles for different engine applications. https://doi.org/10.3403/30334069.

Landis, M. (2014). Results of long-time tractor emission and fuel measurements. *Proceedings international conference of agricultural engineering*.

Liu, Z., Ivanco, A., & Filipi, Z. (2015). Naturalistic drive cycle synthesis for pickup trucks. *Journal of Safety Research, 54*(109), e29–e115. https://doi.org/10.1016/j.jsr.2015.06.005

Mattarelli, E., Rinaldini, C. A., Scrignoli, F., Fregni, P., Gaioli, S., Franceschini, G., & Barater, D. (2019). Potential of electrification applied to non-road diesel engines. *SAE Technical Papers, 2019-24–0202*. https://doi.org/10.4271/2019-24-0202

Mattetti, M., Maraldi, M., Lenzini, N., Fiorati, S., Sereni, E., & Molari, G. (2021). Outlining the mission profile of agricultural tractors through CAN-BUS data analytics. *Computers and Electronics in Agriculture, 184*, Article 106078. https://doi.org/10.1016/j.compag.2021.106078

Mattetti, M., Medici, M., Canavari, M., & Varani, M. (2022). CANBUS-enabled activity-based costing for leveraging farm management. *Computers and Electronics in Agriculture, 194*, Article 106792. https://doi.org/10.1016/j.compag.2022.106792

Mattetti, M., Michielan, E., Mantovani, G., & Varani, M. (2022). Objective evaluation of gearshift process of agricultural tractors. *Biosystems Engineering, 224*, 324–335. https://doi.org/10.1016/j.biosystemseng.2022.11.001

McCaffery, C., Yang, J., Karavalakis, G., Yoon, S., Johnson, K. C., Miller, J. W., & Durbin, T. D. (2022). Evaluation of small off-road diesel engine emissions and aftertreatment systems. *Energy, 251*, Article 123903. https://doi.org/10.1016/j.energy.2022.123903

Miller, R. E. (2000). *Optimization: Foundations and applications*. John Wiley & Sons.

Mocera, F. (2021). A model-based design approach for a parallel hybrid electric tractor energy management strategy using hardware in the loop technique. *Vehicles, 3*(1), 1–19. https://doi.org/10.3390/vehicles3010001

Molari, G., Mattetti, M., Lenzini, N., & Fiorati, S. (2019). An updated methodology to analyse the idling of agricultural tractors. *Biosystems Engineering, 187*, 160–170. https://doi.org/10.1016/j.biosystemseng.2019.09.001

Moreda, G. P., Muñoz-García, M. A., & Barreiro, P. (2016). High voltage electrification of tractor and agricultural machinery – a review. *Energy Conversion and Management, 115*, 117–131. https://doi.org/10.1016/j.enconman.2016.02.018

Perozzi, D., Mattetti, M., Molari, G., & Sereni, E. (2016). Methodology to analyse farm tractor idling time. *Biosystems Engineering, 148*, 81–89. https://doi.org/10.1016/j.biosystemseng.2016.05.007

Pessina, D., & Facchinetti, D. (2009). *Gemelli diversi* (pp. 44–51). Macchine Agricole luglio.

Pieke, C., Stark, W., Pfister, F., & Schyr, C. (2017). DLG powermix on the dynamometer. *ATZ Offhighway Worldwide, 10*(2), 26–31. https://doi.org/10.1007/s41321-017-0018-3

Qiao, H., Zheng, F., Jiang, H., & Dong, K. (2019). The greenhouse effect of the agriculture-economic growth-renewable energy nexus: Evidence from G20 countries. *Science of the Total Environment, 671*, 722–731. https://doi.org/10.1016/j.scitotenv.2019.03.336

Rahman, S. M. A., Masjuki, H. H., Kalam, M. A., Abedin, M. J., Sanjid, A., & Sajjad, H. (2013). Impact of idling on fuel consumption and exhaust emissions and available idle-reduction technologies for diesel vehicles – a review. *Energy Conversion and Management, 74*, 171–182. https://doi.org/10.1016/j.enconman.2013.05.019

Rossi, C., Pontara, D., Falcomer, C., Bertoldi, M., & Mandrioli, R. (2021). A hybrid–electric driveline for agricultural tractors based on an e-CVT power-split transmission. *Energies, 14*(21). https://doi.org/10.3390/en14216912. Articolo 21.

SAE. (2013). *Vehicle application layer* (pp. 1–1255) (j1939-71.

Saetti, M., Mattetti, M., Varani, M., Lenzini, N., & Molari, G. (2021). On the power demands of accessories on an agricultural tractor. *Biosystems Engineering, 206*, 109–122. https://doi.org/10.1016/j.biosystemseng.2021.03.015

Samuelsson, T., Filla, R., Frank, B., & Skogh, L. (2016). Selecting representative working cycles from large measurement data sets. *CVT 2016 commercial vehicle technology symposium, Kaiseralutern, Germany*. https://doi.org/10.13140/RG.2.1.3905.7049

Scolaro, E., Beligoj, M., Estevez, M. P., Alberti, L., Renzi, M., & Mattetti, M. (2021). Electrification of agricultural machinery: A review. *IEEE Access, 9*, 164520–164541. https://doi.org/10.1109/ACCESS.2021.3135037

Troncon, D., Alberti, L., & Mattetti, M. (2019). A feasibility study for agriculture tractors electrification: Duty cycles simulation and consumption comparison. In *2019 IEEE transportation electrification conference and expo (ITEC)* (pp. 1–6). https://doi.org/10.1109/ITEC.2019.8790502

Ullman, T. L., Webb, C. C., Jackson, C. C., & Doorlag, M. H. (1999). Nonroad engine activity analysis and transient cycle generation. https://doi.org/10.4271/1999-01-2800.

UNECE. (2010). *Global technical regulation No. 11—engine emissions from agricultural and forestry tractors and from non-road mobile machinery (ECE/TRANS/180/Add.11/Appendix 2)*.

U.S. Environmental Protection Agency. (2004). *Final regulatory analysis: Control of emissions from nonroad diesel engines (EPA420-R-04–007)*.

Varani, M., Mattetti, M., Molari, G., Biglia, A., & Comba, L. (2023). Correlation between power harrow energy demand and tilled soil aggregate dimensions. *Biosystems Engineering, 225*, 54–68. https://doi.org/10.1016/j.biosystemseng.2022.11.008

Varani, M., Perez Estevez, M. A., Renzi, M., Alberti, L., & Mattetti, M. (2022). Controlling idling: A ready-made solution for reducing exhaust emissions from agricultural tractors. *Biosystems Engineering, 221*, 283–292. https://doi.org/10.1016/j.biosystemseng.2022.07.011